JOURNAL OF GEOPHYSICAL RESEARCH, VOL. 107, NO. B9, 2179, doi:10.1029/2001JB000162, 2002

Topographic outcomes predicted by stream erosion models: Sensitivity analysis and intermodel comparison

G. E. Tucker
School of Geography and the Environment, Oxford University, Oxford, UK

K. X. Whipple
Department of Earth, Atmospheric, and Planetary Sciences, Massachusetts Institute of Technology, Cambridge, Massachusetts, USA

Received 15 January 2001; revised 22 September 2001; accepted 27 September 2001; published 10 September 2002.

[1] Mechanistic theories of fluvial erosion are essential for quantifying large-scale orogenic denudation. We examine the topographic implications of two leading classes of river erosion model, detachment-limited and transport-limited, in order to identify diagnostic and testable differences between them. Several formulations predict distinctly different longitudinal profile shapes, which are shown to be closely linked to terrain morphology. Of these, some can be rejected on the basis of unrealistic morphology and slope-area scaling. An expression is derived for total drainage basin relief and its apportionment between hillslope and fluvial components. Relief and valley density are found to vary with tectonic forcing in a manner that reflects erosion physics; these properties therefore constitute an additional set of testable predictions. Finally, transient responses to tectonic perturbations are shown to depend strongly on the degree of nonlinearity in the incision process. These findings indicate that given proper constraints, fluvial erosion theories can be tested on the basis of observed topography. *INDEX TERMS:* 1824 Hydrology: Geomorphology (1625); 1625 Global Change: Geomorphology and weathering (1824, 1886); 3210 Mathematical Geophysics: Modeling; 8110 Tectonophysics: Continental tectonics—general (0905); *KEYWORDS:* Landscape evolution, topography, geomorphology, erosion, streams, relief

Citation: Tucker, G. E., and K. X. Whipple, Topographic outcomes predicted by stream erosion models: Sensitivity analysis and intermodel comparison, *J. Geophys. Res.*, *107*(B9), 2179, doi:10.1029/2001JB000162, 2002.

1. Introduction

[2] River erosion is one of the primary agents of landscape evolution. Outside of glaciated regions, rivers are responsible for sculpting uplifted terrain into arborescent valley networks and creating the relief that drives gravitational transport processes such as landsliding. Thus quantifying the dynamics of river erosion is a central issue not only in developing models of long-term landscape evolution but also for interpreting the significance of erosional topography and of thermochronologic data [e.g., *Cockburn et al.*, 2000], for deducing controls on sediment supply [e.g., *Tucker and Slingerland*, 1996], and for testing hypothesized interactions between erosional unloading and the dynamics of mountain belts [e.g., *Molnar and England*, 1990; *Beaumont et al.*, 1992; *Willett et al.*, 1993; *Whipple et al.*, 1999].

[3] Recently, a number of different mechanistic theories of long-term river profile development have been proposed [*Howard and Kerby*, 1983; *Snow and Slingerland*, 1987; *Willgoose et al.*, 1991; *Beaumont et al.*, 1992; *Seidl and Dietrich*, 1992; *Sklar and Dietrich*, 1998; *Slingerland et al.*, 1997; *Whipple and Tucker*, 1999]. Though the forms of these various models differ in many important respects, they share the common theme of representing the long-term (hundreds to millions of years) average, reach-scale rate of channel erosion (or deposition) as a function of key controlling factors such as channel gradient, water discharge (or drainage area as a surrogate), sediment flux, and lithology. Yet the underlying premises and assumptions vary, sometimes considerably, among the different proposed erosion formulations. For example, the long-term average rate of stream channel incision has been variously modeled as a function of excess shear stress [e.g., *Howard and Kerby*, 1983; *Howard*, 1994; *Tucker and Slingerland*, 1997; *Whipple et al.*, 2000], total stream power [e.g., *Seidl and Dietrich*, 1992], or stream power per unit bed area [e.g., *Whipple and Tucker*, 1999]. In each of these cases, variation in sediment supply is considered a second-order effect. Alternatively, a number of "transport-limited" models have been proposed, in which an infinite supply of mobile sediment is assumed, so that transport capacity and supply are exactly balanced [e.g., *Snow and Slingerland*, 1987; *Willgoose et al.*, 1991]. Finally, other "hybrid" models have been proposed to account for the role of sediment flux, either in controlling transitions between channel types [e.g.,

0148-0227/02/2001JB000162$09.00

Howard, 1994; *Tucker and Slingerland*, 1997] or in controlling the rate of particle detachment from a resistant substrate [e.g., *Beaumont et al.*, 1992; *Sklar and Dietrich*, 1998; *Slingerland et al.*, 1997; *Whipple and Tucker*, 2002].

[4] Each of these formulations has a basis in theory or experiment or both. Many have been used in the context of modeling three-dimensional landscape structure, and perhaps not surprisingly, all have been shown to succeed at the elementary goal of generating branching drainage networks. The appeal of being able to simulate landforms using simple erosion ''rules'' has stimulated the application of such models to problems ranging from theoretical studies of drainage basin morphology [e.g., *Willgoose et al.*, 1991; *Chase*, 1992; *Howard*, 1994; *Tucker and Bras*, 1998] and to examination of erosion-tectonic feedbacks [e.g., *Beaumont et al.*, 1992; *Whipple et al.*, 1999] and analyses of landscape evolution in particular regions of the world [e.g., *Gilchrist et al.*, 1994; *Tucker and Slingerland*, 1996; *Howard*, 1997; *Densmore et al.*, 1998; *van der Beek and Braun*, 2000; *Snyder et al.*, 2000a]. Ultimately, the formulation and confirmation of such models will constitute an important cornerstone of a ''standard model'' in theoretical geomorphology. Before that can be achieved, however, there remain a number of fundamental unresolved questions that must be addressed in order to test and refine the present generation of long-term river erosion laws. These include questions such as: What are the large-scale morphologic implications of the present generation of models, either under steady state or transient conditions? Are these implications consistent with observed topography? Are there morphologic properties that are sufficiently diagnostic as to discriminate between competing models and to reject some on the basis of observed topography? Can we identify critical physical parameters whose role should be further investigated via field and laboratory studies?

[5] In this paper, we use numerical simulations to address these questions in the context of the widely used ''stream power'' model and its relatives. In particular, we explore their implications for three related issues: (1) the relation between stream profile shape and three-dimensional (3-D) landscape morphology, (2) the relation between relief, drainage density, and tectonic uplift rate in active mountain systems, and (3) the nature of transient responses. The answers to these questions yield testable predictions regarding the large-scale texture of fluvially sculpted terrain that may help to discriminate between alternative models and allow us to reject some in favor of others on the basis of observable topographic forms. We begin by briefly reviewing several of the most common river erosion models and their physical basis. We then analyze the behavior of these models in terms of equilibrium morphology and responses to tectonic input. The analysis in this paper is restricted to the detachment-limited and transport-limited end-member models. *Whipple and Tucker* [2002] extended the analysis to include a hybrid class of models which explicitly incorporates the role of sediment flux in mediating rates of bedrock channel incision.

2. Background: Long-Term Fluvial Erosion Models

[6] We consider two general end-member types of erosion law: the so-called detachment-limited family of models, in which the rate of stream incision is presumed to depend only on local bed shear stress (or a similar quantity), and the so-called transport-limited family of models, in which the sediment flux is equated with the local transport capacity, such that the rate of channel erosion (or deposition) is controlled by along-stream variations in transport capacity. We also briefly review a third category of hybrid models, which are discussed in greater detail by *Whipple and Tucker* [2002]. In view of the many different formulations that have been proposed during the past several years, we do not attempt a thorough sensitivity analysis of all of these stream erosion laws, but rather we restrict attention to two of the most basic (and most widely used) laws. Many of the conclusions we draw, however, are general and can be applied to other classes of model.

2.1. Detachment-Limited Models

[7] The most commonly used stream erosion law [from *Howard*, 1980] takes the form of a power law relationship between stream incision rate, drainage area (as a surrogate for water discharge and possibly sediment flux), and channel gradient:

$$\frac{\partial h}{\partial t} = -KA^m S^n, \tag{1}$$

where h is the elevation of a stream channel relative to the underlying rock column, t is time, S is channel gradient, A is drainage area, and K is an erosional efficiency factor that lumps information related to lithology, climate, channel geometry, and perhaps sediment supply [*Howard et al.*, 1994; *Whipple and Tucker*, 1999]. Depending on the value of exponents m and n, equation (1) can be variously used to represent bed shear stress ($m \simeq 0.3$, $n \simeq 0.7$) [*Howard and Kerby*, 1983; *Howard et al.*, 1994; *Tucker and Slingerland*, 1997], stream power per unit channel length ($m \simeq n = 1$) [*Seidl and Dietrich*, 1992], or stream power per unit bed area ($m \simeq 0.5$, $n \simeq 1$) [*Whipple and Tucker*, 1999]. We refer to these three variations collectively as the stream power family of models and to equation (1) as the generalized stream power law. A fundamental assumption behind the generalized stream power law is that the rate of vertical lowering of a channel bed is limited by the rate at which bed particles can be detached via processes such as abrasion and plucking [e.g., *Foley*, 1980; *Whipple et al.*, 2000] rather than by the rate at which detached particles can be transported. In principle, the effects of sediment flux can be represented by incorporating a sediment flux function as a multiplicative factor in K [*Whipple and Tucker*, 2002]. In practice, however, K is usually treated as a constant, implying that sediment supply effects are either ignored or are subsumed in the exponents. Here we consider only cases of constant K (see *Whipple and Tucker* [2002] for analysis of sediment flux dependency in models like equation (1)). A further assumption in equation (1) is that detachment thresholds (analogous to grain entrainment thresholds in sediment transport theory) are negligible, though this assumption can be easily relaxed [e.g., *Howard*, 1994; *Tucker and Slingerland*, 1997; *Tucker and Bras*, 2000; *Snyder et al.*, 2000b].

[8] Equation (1) takes the form of a nonlinear kinematic wave equation (notice that $S = -dh/dx$, where x is streamwise distance). Unlike formulations that explicitly incorporate sediment flux, the erosion rate at a point is independent

of erosion or transport rates elsewhere in the catchment. These properties have important implications for the style of landscape development, in particular, the nature of transient responses to perturbations in tectonics or climate, as illustrated below and by *Whipple and Tucker* [2002].

2.2. Transport-Limited Models

[9] Transport-limited erosion laws arise from the assumption that the rate of surface lowering is limited by the rate at which sediment particles can be transported away, as in the idealized case of a pile of loose sand and gravel subject to overland flow. In the most basic transport-limited model the fluvial sediment transport capacity, Q_c (L^3/T) is cast as a power function of slope and drainage area (again as a proxy for flood discharge [cf. *Willgoose et al.*, 1991]),

$$Q_c = A^{m_t} S^{n_t}, \tag{2}$$

where the transport efficiency factor K_t is a function of grain size and density, climate/hydrology, channel geometry, and bed roughness. Equating volumetric total transport rate, Q_s, with capacity, and imposing continuity of mass,

$$\frac{\partial h}{\partial t} = -K_t \frac{\partial}{\partial x}[(A^{m_t} S^{n_t})/W], \tag{3}$$

where W is channel width (note that sediment bulk density is usually lumped into K_t). Interestingly, steady state channel profile shapes predicted by equations (1) and (3) can be essentially indistinguishable [*Willgoose et al.*, 1991; *Howard*, 1994; *Tucker and Bras*, 1998]. The presence of a strong diffusive component in equation (3), however, leads to markedly different transient behavior between the two models [*Tucker and Slingerland*, 1994; *Whipple and Tucker*, 2002, Figures 7 and 8]. Furthermore, the nonlocal property of equation (3), i.e., the dependence on sediment flux originating upstream, implies a high degree of sensitivity to fluctuations in the supply of sediment from hillslopes.

2.3. Hybrid Models

[10] Several models have been proposed that are intermediate between these two end-member cases in the sense that they attempt to represent both sediment transport and detachment of resistant material. Here we briefly review these models. More detailed consideration of hybrid models, and in particular the role of sediment flux as a control on bedrock incision rate, is given by *Whipple and Tucker* [2002].

[11] The simplest hybrid model is one that limits the rate of vertical erosion to the lesser of detachment capacity (equation (1)) or surplus transport capacity (equation (3)) [e.g., *Tucker and Slingerland*, 1994]. Under a steady discharge this approach implies an abrupt transition between detachment-limited (''bedrock'') and transport-limited (''alluvial'') channels [e.g., *Howard*, 1994; *Montgomery et al.*, 1996; *Tucker and Slingerland*, 1997]. Under steady state the transition point occurs where the gradient needed to incise at a given rate equals the gradient needed to transport sediment generated by upstream erosion at that same rate [*Tucker et al.*, 2001b, Figure 8]. As discussed by *Whipple and Tucker* [2002], the direction of movement of the transition point in response to tectonic or climatic perturbations depends on the relative degrees of nonlinearity in the sediment transport and bedrock detachment processes (i.e., the relative values of n and n_t in equations (1) and (2), respectively). Note also that under a variable flow regime the transition between channel types is gradational provided $n \neq n_t$ [*Tucker et al.*, 2001b].

[12] *Beaumont et al.* [1992] describe a model in which the stream incision rate, by analogy to a chemical reaction, depends linearly on the imbalance between sediment supply and transport capacity. Similar concepts have been proposed for soil erosion by overland flow [*Foster and Meyer*, 1972]. *Sklar and Dietrich* [1998] and *Slingerland et al.* [1997] present models in which sediment plays the dual, and opposing, roles of abrading bedrock and of shielding the bed from abrasion. The implications of these alternative forms are explored by *Whipple and Tucker* [2002] and will not be considered further here.

[13] Finally, it should be noted that for high-gradient mountain channels it has been argued that debris flows may dominate bed incision [*Seidl and Dietrich*, 1992; *Sklar and Dietrich*, 1998; *Stock and Dietrich*, 1999]. Given the unsteady nature and nonlinear rheology of debris flows and their long recurrence intervals, the mechanics behind the derivation of ''standard'' fluvial theories such as equations (1) and (3) are unlikely to be applicable to such situations.

3. Stream Profiles and 3-D Topography

[14] We first examine the implications of the detachment-limited (equation (1)) and transport-limited (equation (3)) erosion laws in terms of stream profile shape and three-dimensional drainage basin morphology. A well-known implication of equations (1) and (3) is that under conditions of spatially uniform denudation rate, both imply a power law relationship between channel gradient and drainage area:

Detachment-limited

$$S = \left(\frac{U}{K}\right)^{\frac{1}{n}} A^{-\theta_d}, \quad \theta_d = \frac{m}{n} \tag{4}$$

Transport-limited

$$S = \left(\frac{U}{\beta K_t}\right)^{\frac{1}{n_t}} A^{-\theta_t}, \quad \theta_t = \frac{m_t - 1}{n_t}, \tag{5}$$

where U is the vertical erosion rate (L/T), equal to uplift rate in the case of steady state under uniform uplift, and β represents the fraction of eroded material that is transported as particulate sediment load (i.e., either bed load or bed load plus suspended load) [*Willgoose et al.*, 1991; *Howard*, 1994; *Tucker and Bras*, 1998; *Whipple and Tucker*, 1999]. For reasons that will become clear below, θ_d and θ_t are directly related to longitudinal stream profile concavity and are thus referred to here as intrinsic concavity indices. (Here θ_d and θ_t refer to the theoretical intrinsic concavities, while θ refers to an observed concavity index [$S \propto A^{-\theta}$] obtained by regression from slope-area data). The implied power law slope-area relationship is supported by numerous data sets, summarized in Table 1. Concavity indices ranging from <0.3 to >1.0 have been documented, though most values fall in the range 0.4–0.7. Concavity values tend to be the lowest (~0.1–0.3) in low-relief alluvial basins and badlands

Table 1. Reported Values of Concavity Index (θ) in Different Drainage Basins

Location	Concavity Index	Area, km^2
Middle River, Appalachians, Virginia (three branches)[a]	0.64, 0.59, 0.49	
North River, Appalachians, Virginia (four branches)[a]	0.43, 0.47, 0.56, 0.52	
Walnut Gulch, Arizona[b]	0.29	23
Brushy Creek, Alabama[b]	0.53	322
Buck Creek, northern California[b]	0.48	606
Big Creek, Idaho[b]	0.51	147
North Fork Coeur d'Alene River, Idaho[b]	0.47	440
St. Joe River, Idaho[b]	0.47	2,834
St. Regis River, Montana[b]	0.55	787
East Delaware River, New York[b]	0.55	933
Schoharie Creek, New York[b]	0.43	2,408
Moshannon Creek, Pennsylvania[b]	0.58	325
Racoon Creek, Pennsylvania[b]	0.51	448
Montgomery Fork, Tenneessee[b]	0.85	37
Siuslaw, Umpqua, and Alsea River basins, OR[c]	1	0.016–409 (tributary basins)
Mahantango Creek, Pennsylvania[d]	0.49	426
Central Zagros Mountains, Iran[d]	0.42	~120,000
Upper Noyo River, California[e] (seven subbasins)	0.56–1.13 (mean = 0.76)	5.4–64.7 (mean = 21)
Central Range, Taiwan (four basins)[f]	0.41 +/− 0.1	
Coastal basins, northern California (21 basins)[g]	0.25–0.59 (mean = 0.43)	4.1 – 20.8
Waipaoa River, New Zealand (five subbasins)[h]	0.49–0.61	(mean = 0.55)
Enza River, northern Apennines, Italy[i]	0.56	
Virginia badlands[j]	0.19	13 hectares
Utah badlands[j]	0.24	
Great Plains[j]	0.30	
Ephemeral, New Mexico[j]	0.15	
Ephemeral, New Mexico[j]	0.11	

[a] *Hack* [1957].
[b] *Tarboton et al.* [1991].
[c] *Seidl and Dietrich* [1992].
[d] *Tucker* [1996].
[e] *Sklar and Dietrich* [1998].
[f] *Whipple and Tucker* [1999].
[g] *Snyder et al.* [2000a].
[h] *Whipple and Tucker* [2002].
[i] P. Talling (unpublished data, 2001).
[j] Alluvial channel data compiled by *Howard* [1980].

alluvial channels [*Howard*, 1980] (see Table 1). Direct comparison between observed concavity indices and the exponent terms in equations (4) and (5) is only strictly valid for basins that are known (or presumed) to have spatially uniform erosion rates (as would be expected, for example, under the condition of a steady state balance between erosion and spatially uniform uplift) and uniform lithology.

[15] Equations (4) and (5) do not, by themselves, describe the predicted shape of a channel profile or drainage basin. However, it is possible to combine equations (4) and (5) with Hack's law, an empirical drainage network geometry relationship of the form

$$A = k_a x^h \tag{6}$$

and integrate to solve for the shape of a stream profile under different values of theta [*Whipple and Tucker*, 1999] (Figure 1). The concavity of the resulting profiles depends strongly on θ, with channel gradient changing downstream as $S \propto x^{-\theta h}$. We might expect a relationship to exist between stream profile shape and the texture of the landscape as a whole, but what is the nature of that relationship?

[16] To answer this question, we use a numerical model to integrate equation (1) in two dimensions for a landscape undergoing spatially uniform uplift. The numerical model (GOLEM [*Tucker and Slingerland*, 1996]) represents a terrain surface as a matrix of cells. Here three processes are modeled: (1) downslope movement and aggregation of water is represented by routing water at each cell downslope in the direction of steepest descent toward one of eight neighboring cells; (2) the rate of stream incision at each cell is computed from equation (1); and (3) landsliding is represented by imposing an upper limit to hillslope gradient [e.g., *Burbank et al.*, 1994]. The landsliding process governs the hillslope-channel transition and imparts a spatial scale to the model.

[17] Figure 2 compares three steady state simulations under different values of the intrinsic concavity index. In each case, the boundary condition consists of a constant rate of uplift relative to a fixed boundary (representing a hypothetical vertical fault or shoreline) at the lower grid edge. To ensure similarity in spatial scale, the threshold hillslope angle is adjusted such that the hillslope length is the same in each case [*Tucker and Bras*, 1998]. The striking differences between the three cases reveal a close relationship between stream profile concavity and 3-D landscape texture. That the two are related is not surprising, since it is known from theoretical studies of fractal terrain properties [*Rodriguez-Iturbe and Rinaldo*, 1997], stream capture [*Howard*, 1971], and landscape evolution [*Howard*, 1994] that slope-area scaling is linked with drainage network organization. The

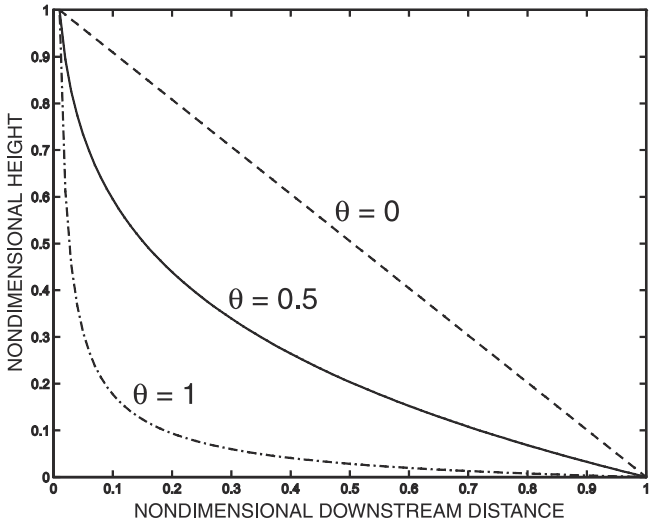

Figure 1. Stream profile concavity as a function of θ. Curves show solutions to equation (4) (or, equivalently, equation (5)) using Hack's law [*Rigon et al.*, 1996] (equation (6)), with $h = 0.6$. Curves are normalized by their maximum height at $x = x_c = 0.01$.

significance of this fact for tectonic geomorphology has not, however, been widely appreciated.

[18] The smoothness of the landscape under small θ is a direct reflection of the near linearity of channel profiles, which facilitates stream capture and integration. By contrast, the extreme roughness and network tortuosity of the simulated terrain under $\theta = 1$ reflects a strong sensitivity to initial conditions, which here consisted of low-amplitude, uncorrelated random noise.

[19] Although each of the three cases in Figure 2 exhibits branching networks and hillslope-valley topography, the structure of the predicted terrain depends quite strongly on the concavity index, which in turn is a direct reflection of the erosion physics. Interestingly, each of these three variants (or their near equivalent) has been used in landscape simulations and has a basis in theory or experimental data. The case in Figure 2a, for example, is typical of the results one would expect under three common (and not apparently unreasonable) assumptions: (1) the fluvial system is transport-limited, (2) sediment transport capacity can be modeled as a function of bed shear stress to the 1.5 power with a negligible entrainment threshold (which leads to $m_f \simeq n_f \simeq 1$ in equation (5) or, equivalently, $\theta \simeq 0$) [e.g., *Chase*, 1992; *Kooi and Beaumont*, 1994; *Tucker and Slingerland*, 1994], and (3) sediment is homogeneous [cf. *Gasparini et al.*, 1999]. Yet the logical outcome of these three hypotheses is a terrain that is clearly unlike that of most mountain drainage basins, both in a visual and statistical sense (Table 1). Instead, the predicted low-concavity landscape, with its small river junction angles and low ruggedness, more closely resembles low-relief alluvial drainage basins [*Howard*, 1980].

[20] The moderate-concavity simulation (Figure 2b) corresponds (though nonuniquely) to the hypothesis that the rate of stream incision depends on either shear stress ($m \simeq 0.3$, $n \simeq 0.7$) or unit stream power ($m \simeq 0.5$, $n \simeq 1$) and is not obviously dissimilar from typical mountainous terrain. Note that this by itself does not uniquely support either of these hypotheses since any model in which $\theta \simeq 0.5$ would generate similar equilibrium properties. The high-concavity simulation (Figure 2c) represents the hypothesis that stream incision rate depends on total stream power ($m = n = 1$). This model was proposed by *Seidl and Dietrich* [1992], and its simplicity has made it an attractive model in a number of different studies [e.g., *Seidl et al.*, 1994; *Anderson*, 1994; *Rosenbloom and Anderson*, 1994; *Tucker and Slingerland*, 1994]. Yet the strong weighting on discharge that it implies leads to topography that is surprisingly rugged and to an inhibition of stream capture that promotes a strong sensitivity to initial conditions.

[21] One might argue that the outcomes in Figure 2 are only comparable to real topography that is known to have spatially uniform erosion rates. However, concavity values obtained from slope-area data for the Central Range of Taiwan, an orogen widely believed to have approximately steady state topography, fall within the range of values obtained from other regions (Table 1). The Appalachian rivers in Table 1, for example, are presumably in a state of long-term decline, and yet they show profile forms that are very similar to those in active orogens. This observation suggests that there may not be a great disparity between the concavity of steady state and nonsteady state (e.g., declining) mountain catchments [*Willgoose*, 1994; *Whipple and Tucker*, 2002; *Baldwin et al.*, 2002]. Moreover, while there is certainly a need to identify steady state landscapes in nature (if, indeed, they exist), it is important to recognize that the idealized steady state condition reveals much about the general tendencies of the underlying models.

[22] The results in Figure 2 suggest two important conclusions. First, there is a very close relationship between stream profile concavity and overall drainage basin morphology. Thus the physical parameters that govern profile concavity (m and n in the case of the general stream power law) are not mere details but have fundamental implications for large-scale landscape evolution. Second, not all erosion laws are created equal. Although equifinality makes it impossible to uniquely validate one model on the basis of slope-area statistics alone, the contrasting behavior of the models allows us to reject some in favor of others. In particular, the data in Table 1 and the character of predicted topography (Figure 2) suggest that erosion laws which predict either very low (less than perhaps 0.2) or very high (on the order of 1) values of equilibrium profile concavity are likely to provide poor representations of the dynamics of real mountain stream networks in most parts of the world. These conclusions are not necessarily limited to the detachment-limited and transport-limited erosion laws considered here but apply to any long-term stream erosion law.

4. Scaling of Relief

[23] A fundamental problem in tectonic geomorphology concerns the relationship between rates of tectonic motion and the resulting topographic relief [e.g., *Hurtrez et al.*, 1999; *Whipple and Tucker*, 1999; *Whipple et al.*, 1999; *Ohmori*, 2000; *Snyder et al.*, 2000a]. In the idealized case of an orogen that has reached a quasi-steady balance between rock uplift and denudation [e.g., *Adams*, 1985;

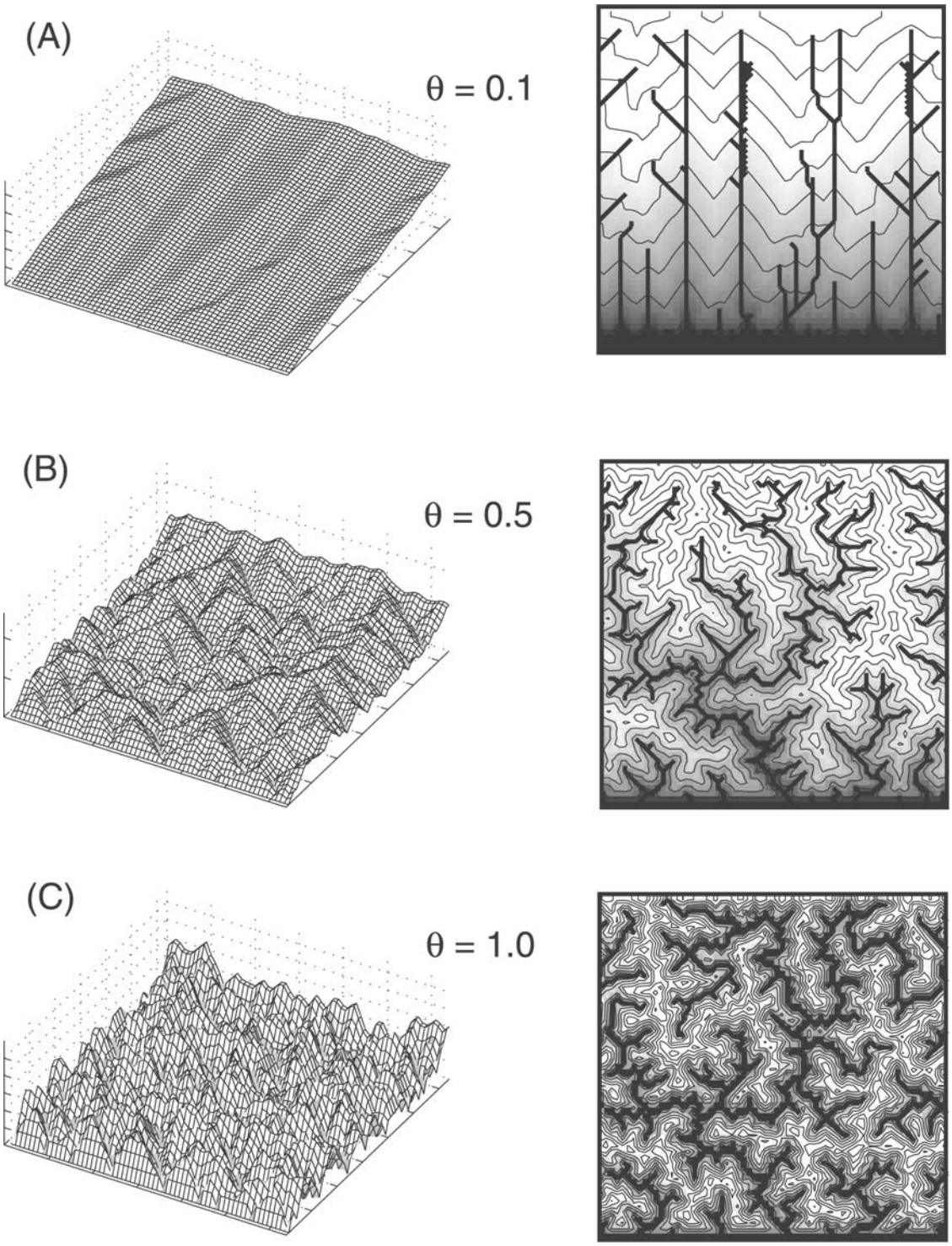

Figure 2. Numerical simulations illustrating the relationship between erosion law parameters, stream profile concavity, and landscape morphology. Each case represents a steady state balance between erosion and steady, uniform uplift relative to a fixed lower boundary. The initial condition consists of a flat surface with low-amplitude uncorrelated random noise superimposed on it. Oblique view of topography and plan view highlighting channels with drainage area greater than an arbitrary threshold are shown for (a) $m = 0.1$, $n = 1$, (b) $m = 0.5$, $n = 1$, and (c) $m = n = 1$. Each simulation represents an area of 6.4 by 6.4 km (64 $\times$ 64 grid cells). Other parameters are $U = 0.001$ m yr^{-1} in all three runs; $K = 0.0025$ $m^{0.8}$ yr^{-1}, 10^{-5} yr^{-1}, and 10^{-8} m^{-1} yr^{-1} in Figures 2a, 2b, and 2c, respectively; and $S_h = 0.14$, 0.58, and 3.33 in Figures 2a, 2b, and 2c, respectively. Note that the extreme tortuosity in Figure 2c arises from a tortuous initial drainage pattern, which reflects the use of an algorithm to route drainage through closed depressions in the initial surface [*Tucker et al.*, 2001c].

Dahlen and Suppe, 1988; *Reneau and Dietrich*, 1991; *Ohmori*, 2000], terrain relief will presumably be controlled by the rate of crustal uplift and by the efficiency of various erosional agents. Beyond this fairly obvious generalization, however, little is known quantitatively about the sensitivity of landscape relief to tectonic forcing. Using the stream power framework, *Whipple and Tucker* [1999] developed a theoretical relationship between rock uplift rate and fluvial relief (defined as the height difference between the upper extent of the channel network and the drainage basin outlet) for a steady state drainage basin. *Snyder et al.* [2000a, 2000b] tested the theory in a region of variable long-term uplift rates and found a correlation between fluvial relief and uplift rate that is consistent with a fairly high degree of nonlinearity in the physics of channel incision, though we believe it is likely that this nonlinearity results from an effective threshold for entrainment and transport of bed material rather than a large value of n. Both studies, however, considered only the channelized portion of the landscape. In this section we extend the theoretical framework to incorporate hillslope relief and variations in drainage density, using the idealized "threshold slope" concept. The 1-D analytical results are tested using 2-D numerical simulations.

[24] Fluvial relief can be expressed as a function of a dimensionless uplift erosion number (N_E) which incorporates rock uplift rate, catchment scale, and factors such as climate, lithology, and basin hydrology. It is defined as

$$N_E = \frac{U_0}{K} k_a^{-m} L^{n-hm} H^{-n}, \tag{7}$$

where U_0 is the spatially averaged uplift rate, L is the total length of the main stream from divide to outlet (i.e., including any hillslope flow path above the channel head), and H is an unspecified characteristic vertical scale (such as mean elevation, if known). Let x denote streamwise distance downstream of the drainage divide. The origin point $x = 0$ is defined as that point along the basin perimeter that has the longest streamwise path length, L, to the outlet point. Fluvial relief is defined as the height difference between the head of the main stream, located at $x = x_c$, and the basin outlet at $x = L$. Following the derivation of *Whipple and Tucker* [1999], fluvial relief for a steady state basin is obtained by substituting equation (6) into equation (4) and integrating upstream. In dimensionless form,

$$R_{*f} = N_E^{1/n} U_*^{1/n} \left(\frac{1-hm}{n}\right)^{-1} \left(1 - x_{*c}^{1-hm/n}\right), \quad \frac{hm}{n} \neq 1 \tag{8a}$$

$$R_{*f} = -N_E^{1/n} U_*^{1/n} \ln x_{*c}, \quad \frac{hm}{n} = 1, \tag{8b}$$

where R_{*f} is dimensionless fluvial relief (height difference between headwaters and outlet divided by a characteristic height scale, H), U_* is dimensionless uplift rate defined by $U_* = U/U_0$ (i.e., local rate U divided by mean U_0, equal to unity under spatially uniform uplift), and $x_{*c} = x_c / L$ is the dimensionless streamwise distance from the drainage divide to the head of the fluvial channel.

[25] The relief equations (8a) and (8b) constitute a field-testable prediction but suffer from two limitations. First, they describes only fluvial relief, which in some cases may constitute 80–90% of total catchment relief [e.g., *Whipple and Tucker*, 1999] but in small catchments (<100 km^2) may be considerably less [*Sklar and Dietrich*, 1998; *Stock and Dietrich*, 1999]; this ratio appears to vary both with catchment scale and from region to region. Second, the drainage density, which appears in the x_{*c} term, is effectively treated as a constant in equations (8a) and (8b). Yet field evidence and theoretical arguments suggest that drainage and valley density, and thus x_{*c}, may vary systematically with relief and are therefore not independent variables [*Kirkby*, 1987; *Montgomery and Dietrich*, 1988; *Howard*, 1997; *Oguchi*, 1997; *Tucker and Bras*, 1998; *Tucker et al.*, 2001a].

[26] To model variations in drainage density in a high-relief, tectonically active setting, we start by assuming that landsliding is the dominant agent of hillslope erosion. A simple but physically reasonable way to model landslide-driven denudation is to assume that there exists a threshold hillslope gradient, S_h, below which the mass movement rate is negligible and above which transport rate becomes effectively infinite [*Carson and Petley*, 1970; *Anderson and Humphrey*, 1990; *Howard*, 1994; *Burbank et al.*, 1994; *Tucker and Slingerland*, 1994; *Schmidt and Montgomery*, 1995; *Densmore et al.*, 1998; *Roering et al.*, 1999]. This simple approximation neglects the stochastic nature of landsliding [e.g., *Densmore et al.*, 1998], and consequently, the threshold gradient is best thought of as an average hillslope gradient about which there will be some natural variability due to heterogeneity in rock properties and the stochastic nature of hillslope failure. Slope length effects are also neglected [*Schmidt and Montgomery*, 1995]. In some cases the failure threshold may vary systematically in space as a function of variables such as pore pressure or lithology; here, however, the threshold is treated as spatially uniform.

[27] Following *Howard* [1997] and *Tucker and Bras* [1998], we can write an expression for the size of a zero-order catchment, A_0, under conditions of spatially uniform surface lowering rate and a spatially constant slope threshold. Substituting the threshold hillslope angle S_h in (4) and solving for the drainage area at which the required channel slope equals the maximum hillslope gradient, we have

$$A_0 = \left(\frac{U}{K}\right)^{\frac{1}{m}} S_h^{-\frac{n}{m}}. \tag{9}$$

Note that A_0 varies directly with uplift rate, which implies that (all else being equal) a higher-relief catchment should have a lower valley density, and vice versa. This inverse relation between relief and valley density for regions with planar, landslide-dominated slopes is a testable prediction. It appears to be supported by data from the badlands in the western United States [*Howard*, 1997] and from Japanese mountains [*Oguchi*, 1997] (Figure 3), though clearly there is a need to extend the analysis to other regions.

[28] The relationship in equation (9) can be used to express x_{*c} as a function of erosion rate (equal to uplift rate under steady state), erosion coefficient (K), and threshold gradient. This requires establishing a relationship between basin length and basin area for a zero-order catchment. *Montgomery and Dietrich* [1992] presented data from unchanneled valleys and low-order basins in the western United States that indicate that the well-known power law relationship between length and area in large river basins extends downward to low-order and zero-order basins. Thus we have some justification for describing the length-area

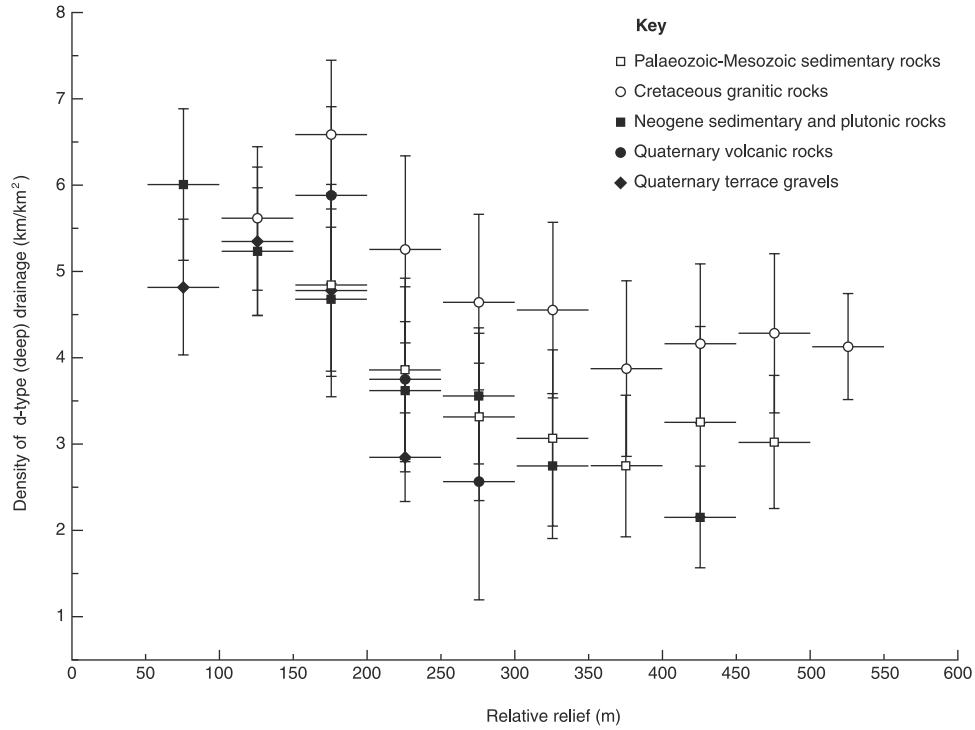

Figure 3. Relationship between relative relief and drainage density for Japanese mountains [see *Oguchi*, 1997]. Relative relief is defined as the difference between maximum and minimum altitudes in a cell of 500 m by 500 m. Symbols indicate lithology; vertical error bars show standard deviation. Plot includes only "d-type" (valley-occupying) drainages, identified on the basis of contour angles <53°; these correspond to V-shaped valleys.

relationship in terms of Hack's law (equation (6)). Small changes in the scaling exponent might be expected as one progresses from channel networks to unchanneled valleys and slopes [*Montgomery and Dietrich*, 1992]; such changes would influence the results only in detail and are not considered further here.

[29] Substituting equation (6) into equation (9), x_{*c} can be written (in dimensionless form)

$$x_{*c} = N_E^{\frac{1}{hm}} U_*^{\frac{1}{hm}} S_{*h}^{-\frac{n}{hm}}, \tag{10}$$

where $S_{*h} = S_h L/H$ is the nondimensional slope threshold. Equation (10) predicts that the upper limit of the fluvial system will vary with (1) the uplift-erosion number, which encapsulates erosion (or uplift) rate, climate, and lithology, and (2) the threshold gradient. The hillslope relief can then be computed as the product of hillslope length, x_c, and threshold gradient, giving

$$R_{*h} = N_E^{\frac{1}{hm}} U_*^{\frac{1}{hm}} S_{*h}^{\frac{1-n}{hm}}, \tag{11}$$

where R_{*h} is dimensionless hillslope relief defined as $R_{*h} = [z(0) - z(x_c)]/H$. Combining equations (8a), (8b), (10), and (11), we can write an expression for total relief as the sum of hillslope and fluvial components:

$$R_{*t} = N_E^{1/n} U_*^{1/n} \left(1 - \frac{hm}{n}\right)^{-1} \left(1 - N_E^{\left(\frac{1}{hm} - \frac{1}{n}\right)} U_*^{\left(\frac{1}{hm} - \frac{1}{n}\right)}\right) \cdot S_{*h}^{\left(1 - \frac{n}{hm}\right)} + N_E^{\frac{1}{hm}} U_*^{\frac{1}{hm}} S_{*h}^{\frac{1-n}{hm}}, \quad \frac{hm}{n} \neq 1 \tag{12a}$$

$$R_{*t} = -N_E^{1/n} U_*^{1/n} \cdot \ln\left(N_E^{\frac{1}{hm}} U_*^{\frac{1}{hm}} S_{*h}^{-1}\right) + N_E^{\frac{1}{hm}} U_*^{\frac{1}{hm}}, \quad \frac{hm}{n} = 1. \tag{12b}$$

Thus total relief is a nonlinear function of the uplift-erosion number. An important caveat is in order here: in deriving hillslope relief we have assumed that there is a direct transition from "fluvial" channels that obey equation (1) to essentially planar, landslide-dominated hillslopes. Some have argued that steep headwater channels in many mountain ranges are dominated by debris flow erosion and should be considered mechanically different from the purely fluvial channels that we have modeled using equation (1). The mechanics of such debris-flow-dominated channels are not well understood, but topographic data and theoretical considerations suggest that debris flow activity may effectively impart a lower threshold gradient to these channels [*Seidl and Dietrich*, 1992], with a gradational transition to purely fluvial channels (Figure 4) [*Stock and Dietrich*, 2002]. We can take some comfort from the observation that in the idealized scenario illustrated in Figure 4, assuming that the transition length between threshold hillslopes and debris flow channels is constant, the slope term in equation (12) would simply become a weighted average of the two thresholds, with the basic scaling behavior unchanged. Since we lack a fully developed mechanistic theory of debris flow channels at present, it seems prudent to relegate this detail to future research; however, it would be straightforward to incorporate a law for debris flow erosion into the relief expression

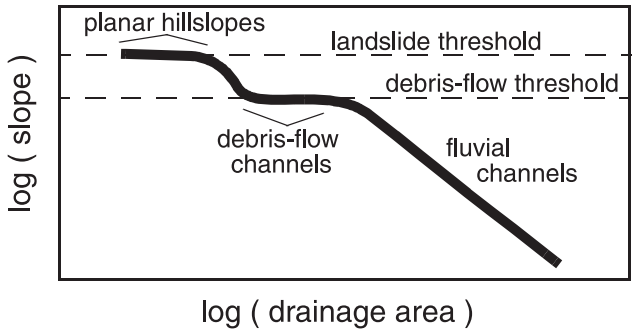

Figure 4. Schematic illustration of slope-area scaling under two slope thresholds, one for the onset of significant debris flow scour and a higher one for planar shallow landsliding.

above, as an intermediate case between fluvial channels and planar hillslopes.

[30] The behavior of equation (12) is illustrated in Figure 5; the default parameters used in this and other figures are listed in Table 2. At low values of the uplift-erosion number (meaning larger catchments, lower uplift/erosion rates, and/or more efficient fluvial erosion), most of the total relief is fluvial relief, and the scaling relationship is close to that derived by *Whipple and Tucker* [1999] for the case of constant x_c. At higher values, however, the role of mass wasting in imposing an upper limit to relief becomes apparent [e.g., *Schmidt and Montgomery*, 1995]. Under higher values of N_E the contribution of hillslope relief to the total becomes increasingly dominant until total relief approaches a maximum value at $R_h / R_t = 1$ (a situation that is seldom observed beyond the scale of an individual hillslope). An important implication of this is that a potential response of mountainous terrain to rapid rock uplift is a reduction in valley density. This is a prediction that can, in principle, be tested in certain tectonically active regions. The best test case would be one in which erosion rates were nearly uniform within individual catchments but varied systematically between catchments. If contrasts in climate and rock type were minimal or could be controlled for, then the stream gradients, relief, and valley density of individual basins could be compared to test equation (12) and to provide quantitative constraints on its physical parameters. Given that the theory has been developed for fluvial-hill-

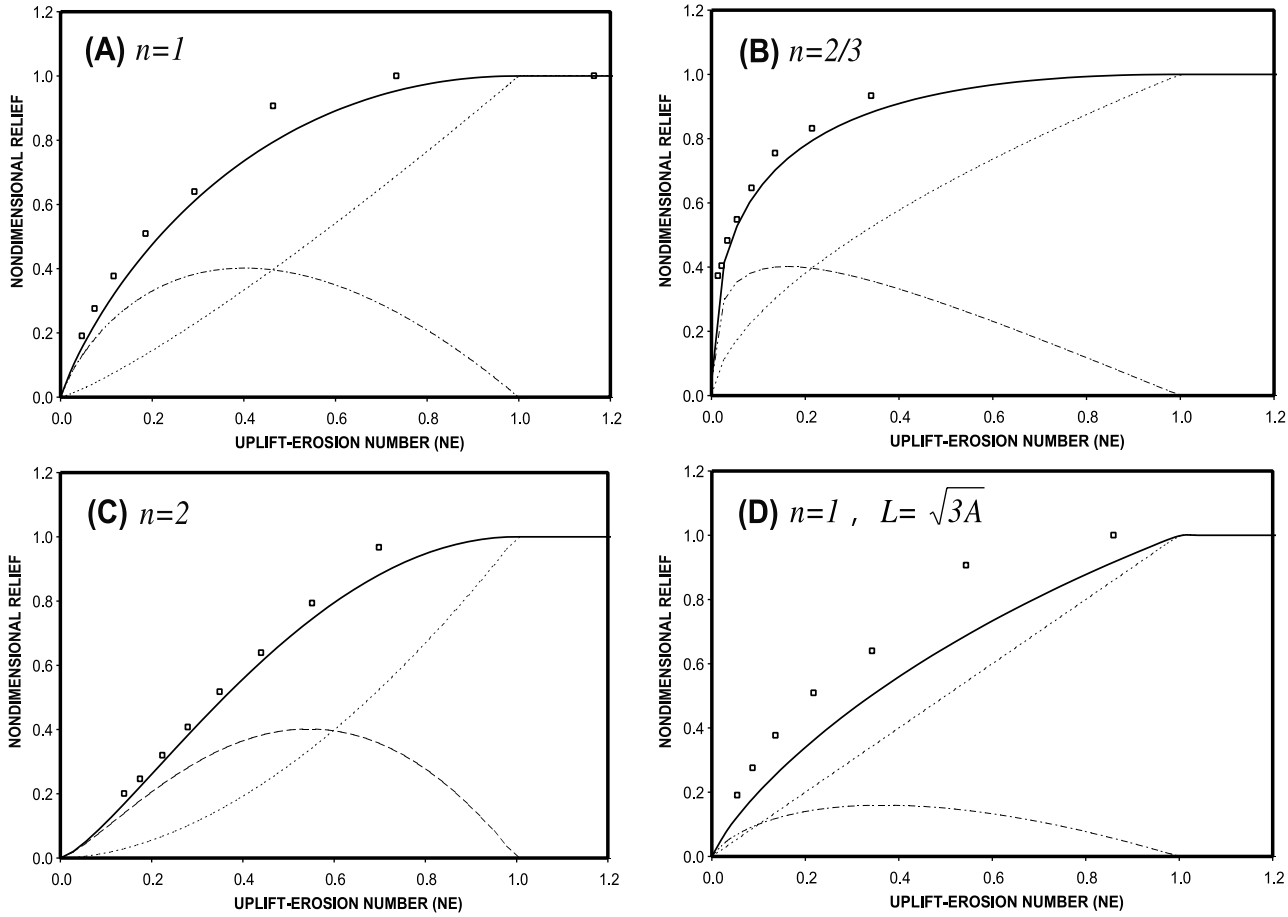

Figure 5. Nondimensional relief as a function of uplift-erosion number (equation (12)). Plot shows fluvial (R_{*f}, dot-dashed), hillslope (R_{*h}, dashed), and total (R_{*t}, solid) relief. Symbols show total relief in 2-D numerical simulations, which is calculated from the average height of the central ridge line (see Figure 6). For (a) n = 1, (b) n = 2/3, (c) n = 2, and (d) n = 1 and using the geometric scaling law [*Montgomery and Dietrich*, 1992].

Table 2. Default Parameter Values used in Figures 5 and 6

Parameter	Value
m/n	0.5
K (n = 1)	10^{-5} yr^{-1}
K (n = 2)	1.6×10^{-8} m^{-1} yr^{-1}
K (n = 2/3)	8.6×10^{-5} m$^{1/3}$ yr^{-1}
L	3200 m
H	3200 m (= LS_h)
S_h	1
h	1.67 (= 1/0.6)
k_a	6.69 m$^{0.33}$
U	10^{-5} to 0.1 m yr^{-1}

Table 3. Rules Applied in Numerical Simulations

Process	Equation or Rule
Surface water routing	Drainage from cell follows steepest descent direction toward one of eight neighboring cells
Fluvial erosion	Equation (1)
Landsliding	Maximum limit to gradient between any two adjacent cells
Tectonic uplift	Spatially uniform relative to fixed boundary

slope transitions, care would need to be taken to avoid glaciated regions and to account for the possible modifying role of debris flows.

[31] Also shown in Figure 5 are the results of numerical experiments designed to test the 1-D analytical theory. Example simulations are shown in Figure 6; in each experiment the GOLEM landscape evolution model [*Tucker and Slingerland*, 1996; *Tucker and Bras*, 1998] was run using the geometry shown in Figure 2, the rule set listed in Table 3, and the default parameters listed in Table 2. No fitting was performed. For each simulation the uplift-erosion number was computed using Hack's law (equation (6)) with either the original empirical parameters derived by *Hack* [1957] (Figures 5a–5c) or with the structural relation $A = (1/3)\,L^2$ of *Montgomery and Dietrich* [1992] (Figure 5d). Though a closer fit could be obtained under smaller values of k_a (which indicates that the numerical model produces narrower catchments than those originally studied by Hack), the important message of Figure 5 is that the 1-D analytical equation (12) provides a good approximation for relief in a 3-D terrain with realistic branching drainage networks. Figure 6 also provides a striking visual illustration of the predicted sensitivity of terrain texture (valley density) to uplift rates (recall that $N_E \propto U$).

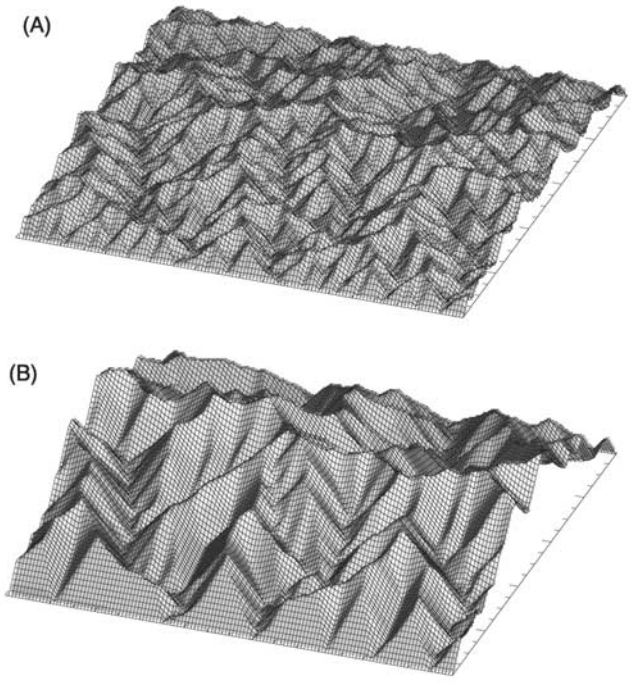

Figure 6. Numerical simulations of mountainous topography under steady, uniform uplift, showing variations in terrain relief and valley density as a function of the uplift-erosion number (N_E). (a) N_E = 0.05 (R_{*t} = 0.19). (b) N_E = 0.12 (R_{*t} = 0.38). In both runs, n = 1. N_E was calculated using Hack's law (equation (6)) and was varied by changing uplift rate (U = 0.001 and 0.0025 m yr^{-1} in Figures 6a and 6b, respectively). Grid size is 128 × 128 cells (grid cell width is 50 m, giving a scale of 6.4 × 6.4 km; ridge height is ~600 and ~1200 m in Figures 6a and 6b, respectively). Other parameters are listed in Table 2.

[32] A further prediction of the total relief equation (12) is that the relative proportions of fluvial and hillslope relief should vary systematically with the uplift-erosion number. On the basis of analyses of digital elevation data, fluvial relief has been observed to constitute from ~40% to ~90% of total catchment relief in basin larger than ~50 km^2 [*Stock and Dietrich*, 1999; *Whipple and Tucker*, 1999]. Figure 7 illustrates this relationship using the parameters in Table 2. In general, fluvial relief dominates under large catchments, low uplift rates, and efficient erosion (high K; for example, highly erosive climate or erodible lithology). Perhaps surprisingly, there is little sensitivity to threshold gradient

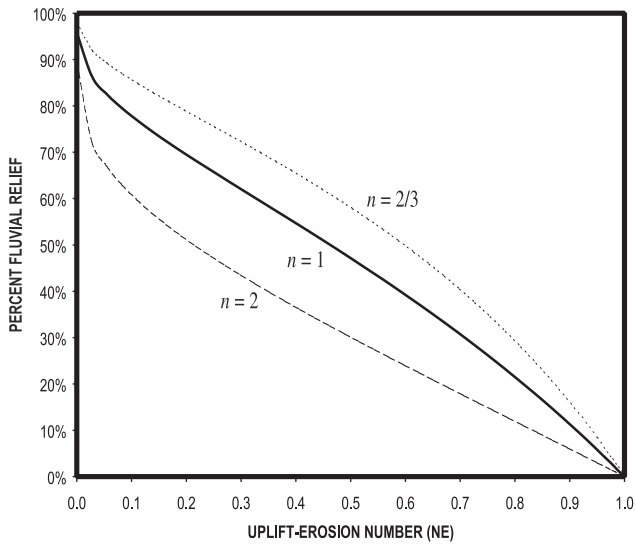

Figure 7. Relative proportions of hillslope and fluvial relief as a function of uplift-erosion number, from equations (11) and (12), for n = 1 (solid), n = 2/3 (short dashed), and n = 2 (long dashed).

because of the contrasting roles of slope length and gradient.

[33] Of the many possible predicted outcomes for total relief, some are clearly invalid, at least at scales larger than that of an individual hillslope. For example, the theory implies that there are potentially conditions under which hillslope relief will constitute all or most of the relief within a mountain range, yet to the best of our knowledge this is rarely observed (except in the obvious case of a single hillslope or first-order catchment). Such failed predictions are especially useful because they can reveal aspects of the models that are oversimplified and provide information about that portion of the parameter space within which nature lies.

5. Transient Responses

[34] The equilibrium states predicted by the detachment-limited (equation (4)) and transport-limited (equation (5)) models can be indistinguishable, depending on θ_d and θ_t. Where cases of approximate steady state topography can be identified in the field [e.g., *Adams*, 1985; *Dahlen and Suppe*, 1988; *Reneau and Dietrich*, 1991; *Ohmori*, 2000], it is possible in principle to calibrate the parameters of either model but not to discriminate between them based on the topography alone. It is in cases of transient response to tectonic or other perturbations that we might expect the dynamics of models like equations (1) and (3) to reveal themselves. In this section, we use numerical simulations to investigate the potential for diagnostic ''signatures'' under conditions of transient response to rapid differential uplift. We focus here on the role of nonlinearity in detachment-limited fluvial systems. *Whipple and Tucker* [2002] examine differences between transport-limited, detachment-limited, and hybrid models under transient response.

5.1. Erosional Waves

[35] A fundamental difference between equations (1) and (3) lies in the wave-like nature of the former and the diffusive nature of the latter [*Whipple and Tucker*, 2002, Figures 8 and 9]. Whereas the transport-limited model is an advection-diffusion equation [e.g., *Paola et al.*, 1992], equation (1) takes the form of a nonlinear kinematic wave equation [*Rosenbloom and Anderson*, 1994; *Whipple and Tucker*, 1999; *Whipple*, 2001; *Royden et al.*, 2000] and can be rewritten as

$$\frac{\partial h}{\partial t} = -KA^m S^{n-1}\left|\frac{\partial h}{\partial x}\right|, \quad \frac{\partial h}{\partial x} < 0, \tag{13}$$

where $C \simeq KA^m S^{n-1}$ is the wave celerity. An obvious prediction of equation (13) is that solutions will take the form of traveling waves. *Whipple and Tucker* [1999] used this wave behavior to derive a timescale of response to tectonic perturbations. A less obvious implication of equation (13) is that the presence and nature of nonlinearity in n have a fundamental impact on the shape of stream profiles during transients. Both numerical [*Tucker*, 1996] and method of characteristics [*Weissel and Seidl*, 1998] solution methods reveal that equation (13) exhibits three distinct classes of transient behavior corresponding to $n < 1$, $n = 1$, and $n > 1$, with shocks appearing in the solution when $n \neq 1$. These modes of behavior are illustrated by finite difference solutions to equation (1) (Figure 8). Under $n = 1$, equation (13) reduces to a linear kinematic wave equation with pure parallel retreat (Figure 8a). For $n < 1$, wave speed is greater on gentler slopes, leading to the pattern shown in Figure 8b in which a singularity (abrupt slope break) appears at the base of the retreating knickpoint. This same behavior occurs in *Howard*'s [1994, 1997] simulation model of badland formation ($n = 0.7$), where it shows up as a slope break at the scarp-pediment boundary. For $n > 1$, wave celerity is greater on steeper slopes, leading to the pattern shown in Figure 8c. Here the singularity appears at the top of the retreating form and the profile below it takes on a smooth, ''graded-like'' morphology. Thus the predicted morphology of channel profiles is diagnostic of the underlying dynamics, which led *Weissel and Seidl* [1998] to conclude that the $n > 1$ case most closely corresponds to the observed morphology of stream profiles along the eastern Australian escarpment. Note, however, that the $n > 1$ case is in some respects nonunique; solutions involving a downstream transition to transport-limited behavior will also produce declining graded profiles [*Whipple and Tucker*, 2002].

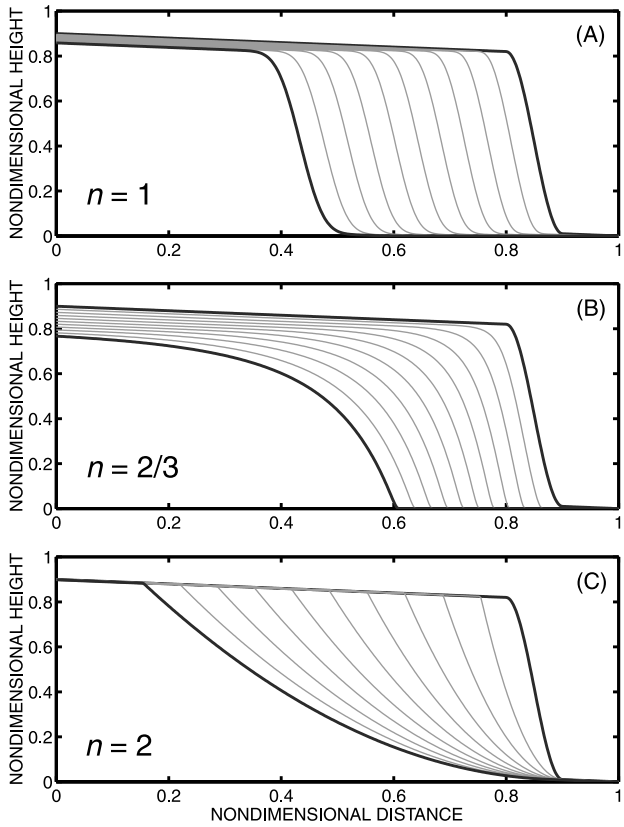

Figure 8. One-dimensional finite difference solutions to equation (1) starting from a hypothetical stream profile with an initial step. Each panel shows several time slices. Discharge is constant along the profile. For (a) $n = 1$, (b) $n = 2/3$, and (c) $n = 2$.

5.2. To Retreat or Not Retreat

[36] When played out in three dimensions, these three modes of behavior have fundamental implications for large-scale patterns of landscape evolution in response to rapid

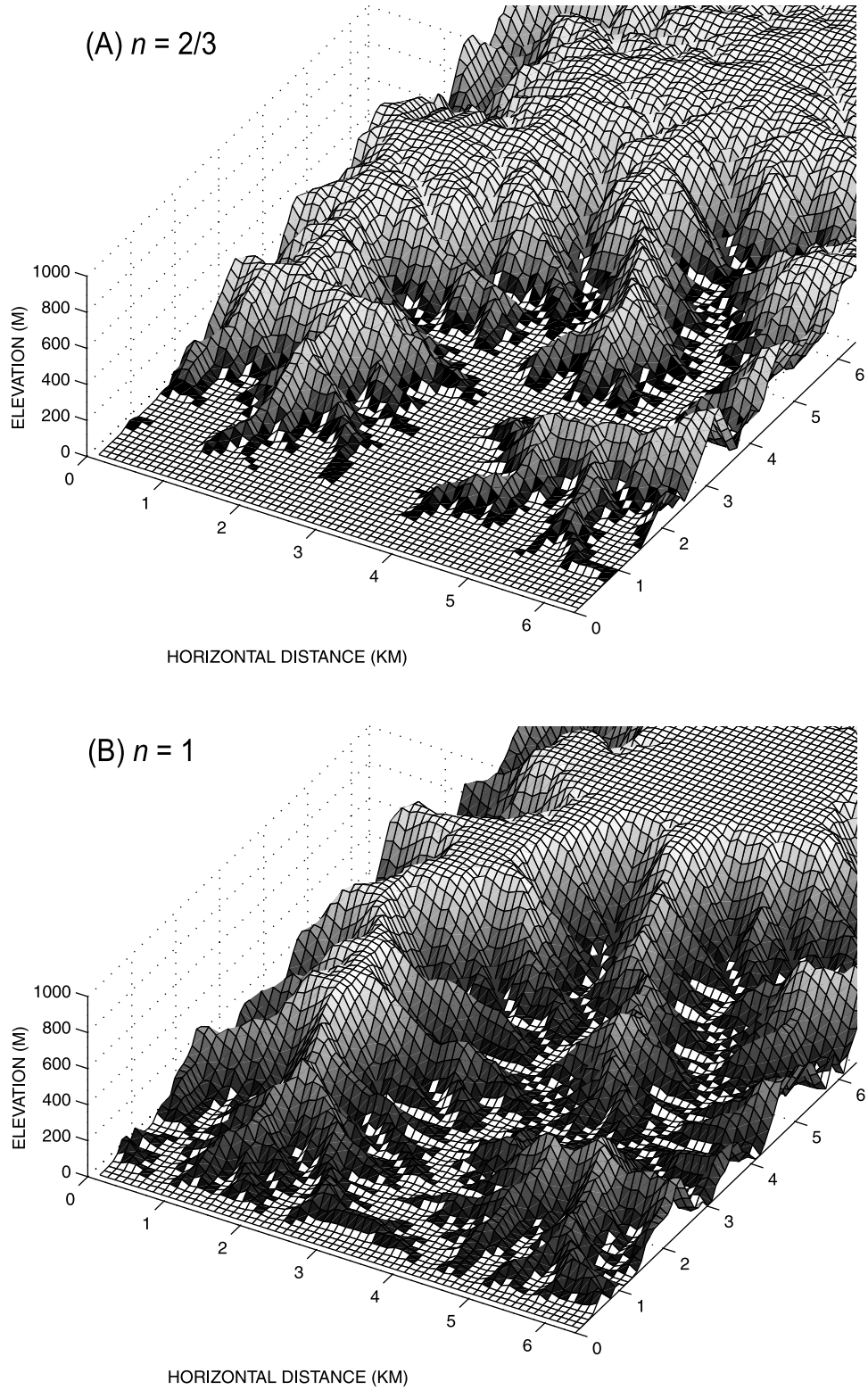

Figure 9. Detachment-limited simulations showing dissection of a plateau under varying degrees of nonlinearity in gradient (n values). Starting condition is a level plateau with a small amount of uncorrelated random noise. Each case represents a stage in which close to 50% of the original mass has been eroded. For (a) $n = 2/3$, (b) $n = 1$, and (c) $n = 2$. Domain size is 64×128 100-m grid cells.

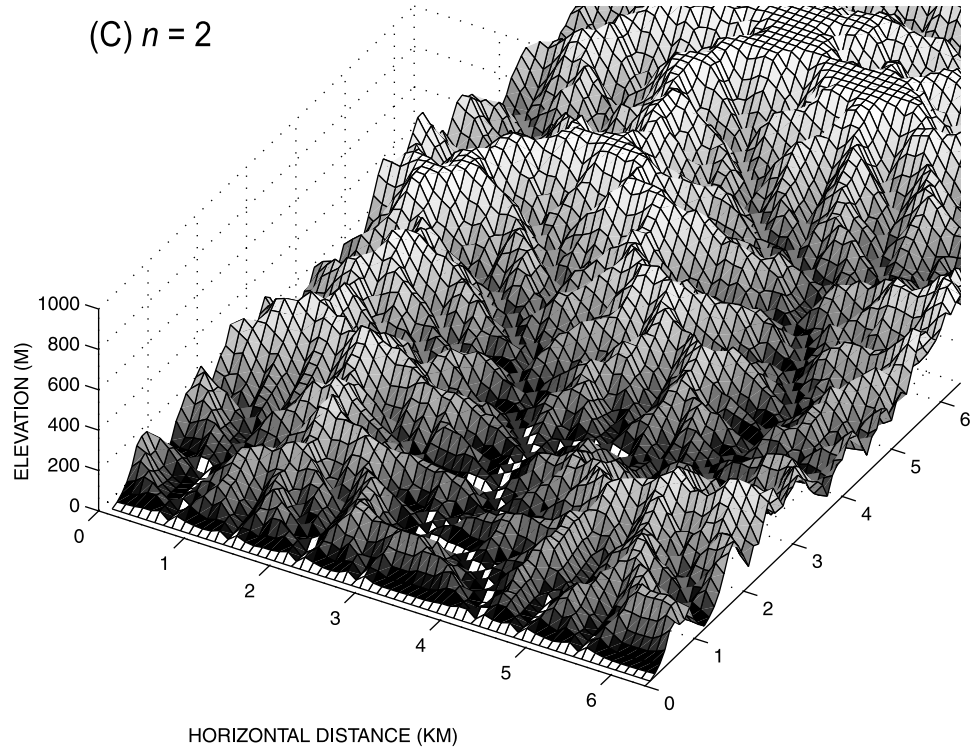

Figure 9. (continued)

differential rock uplift. The pattern of response is illustrated in the simulations shown in Figure 9. Here the initial condition consists of an elevated horizontal plateau with an escarpment at one end and a small quantity of uncorrelated random noise applied to the initial elevation field. The cases $n < 1$ and $n = 1$ both exhibit large-scale escarpment retreat (Figures 9a and 9b). (Note that unlike the cases explored by *Tucker and Slingerland* [1994], the escarpment morphology is sinuous because (1) the plateau is not inclined away from the initial scarp and (2) drainage is forced to exit at the foot of the initial scarp.) The resulting morphology has much in common with the "back wearing" models of landscape evolution championed by *King* [1953] and *Penck* [1921] [see also *Kooi and Beaumont*, 1996]. By contrast, the case $n > 1$ predicts large-scale, distributed denudation without clear escarpment retreat (although wave-like behavior still appears in the form of a sharp upper slope break, just as in the 1-D case; such a feature might, in practice, be called an escarpment) (Figure 9c). The $n > 1$ case therefore more closely resembles *Davis*'s [1899] vision of widespread down wearing following rapid uplift. The timing of the responses is also different. With $n > 1$ the strong weighting of gradient means that the mean rate of denudation slows very quickly as relief is worn down; in the linear and sublinear cases, denudation rate first rises in response to drainage net integration, then gradually declines (Figure 10). Implications of these models for postorogenic relief decline are considered by *Baldwin et al.* [2002].

6. Discussion and Conclusions

[37] Many of the fluvial erosion laws that have been proposed vary considerably in terms of their predicted intrinsic longitudinal profile concavity and therefore in the character of three-dimensional topography. In some cases, seemingly plausible erosion laws imply steady state topography in which the terrain ruggedness and drainage network geometry differ markedly from observed mountain topography. The first part of this analysis has focused on

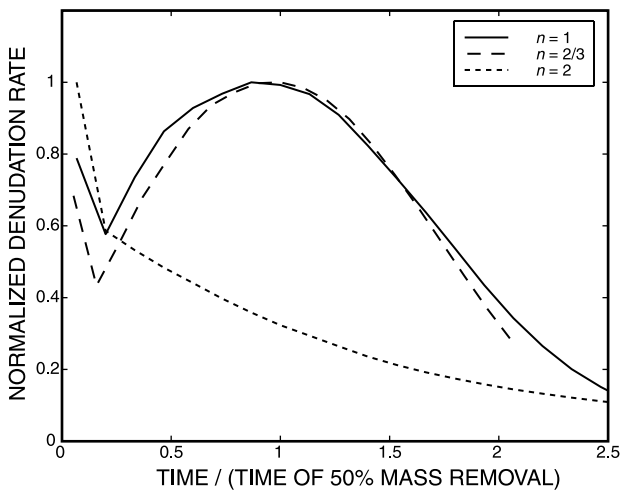

Figure 10. Denudation rate versus time for the three simulations pictured in Figure 9. Timescale is normalized by the time at which 50% of initial mass has been removed; vertical scale is normalized by the maximum rate. The initial spike in each curve represents mass lost to landsliding during the first time step, which reduces the initial plateau edge to the threshold slope gradient.

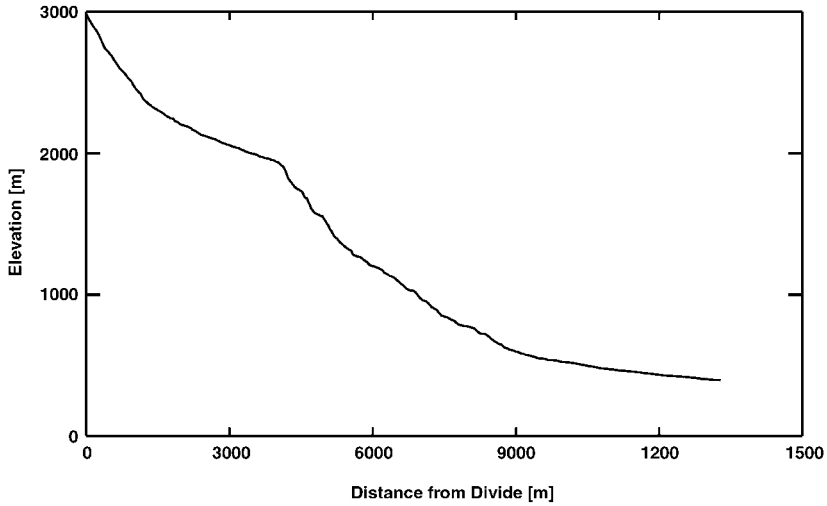

Figure 11. A possible example of a wave-like transient response to an accelerated rate of base level fall. Plot shows the longitudinal stream profile of Pat Keyes Canyon in the Inyo Mountains, along the west flank of the Saline Valley, southeastern California. There are no known lithologic contacts or structural features that coincide with the abrupt change in channel gradient.

steady state forms, and thus strictly speaking, the models are only comparable to such cases in nature. However, scaling properties in purportedly steady state orogens such as Taiwan are similar to those observed worldwide (Table 1), suggesting that a comparison with typical observed drainage basin properties is valid. Thus it is possible to reject certain otherwise plausible erosion models based on their large-scale topographic implications. In particular, the total stream power erosion law ($\partial h / \partial t \propto AS$) appears to be inconsistent with the observed concavity and topography of most mountain drainage basins. The linear transport capacity law ($Q_s \propto AS$) likewise appears to be inconsistent with typical mountain topography, though similar low-concavity transport laws may be applicable to low-relief, transport-limited alluvial drainage networks with fine bed channels [*Howard*, 1980].

[38] There remain a number of erosion laws that yield similar or identical predictions in terms of steady state topography and, in particular, in terms of intrinsic concavity (θ). One aspect in which otherwise similar models may differ is in their predicted scaling relationship between relief and uplift rate (or, more generally, erosion rate). In the case of both transport-limited and detachment-limited models the relief-uplift relationship is governed by the nonlinearity in the gradient term. Here that nonlinearity is described by a single exponent, n (or n_t); however, the basic fact that relief sensitivity is controlled by the gradient term(s) should apply generally to any form of erosion law that contains such a term. Thus, for example, *Snyder et al.* [2000b] found that the addition of a threshold term in equation (1) under stochastic runoff leads to reduced relief-uplift sensitivity as a consequence of the added nonlinearity in channel gradient. The relief-uplift relationship is therefore another prediction that can be tested in settings with variable uplift (or erosion) rates and evidence for quasi-steady state [e.g., *Snyder et al.*, 2000a].

[39] The scaling of total (as opposed to fluvial) relief depends also on the nature and dynamics of hillslope processes. Our analysis suggests that in regions characterized by planar, shallow landsliding above a threshold gradient, total relief will be somewhat less sensitive than fluvial relief to tectonic forcing. The analysis suggests that neither river incision nor landsliding alone provide a "limit" to relief; rather, relief is dictated by the interaction between the two processes. The total relief equation (12) is an additional testable prediction that varies among erosion laws.

[40] Important differences between the erosion laws that we have analyzed arise in cases of transient response to rapid tectonic uplift (or, more generally, base level lowering). The class of transport-limited and detachment-limited models is distinguishable on the basis of the presence or absence of a sharp, headward migrating slope break in response to accelerated base level fall [*Whipple and Tucker*, 2002]. Figure 11 shows a possible example of this type of wavelike response in the Inyo Mountains of southeastern California. Rapid subsidence along the hanging wall of this normal fault block is recorded by the small size of alluvial fans at the front of this steep, faceted range front [*Whipple and Trayler*, 1996]. We suspect that the break in the stream profile records an acceleration in slip rate because there are no known lithologic or structural contacts that coincide with the abrupt change in both channel and hillslope steepness [*California Division of Mines and Geology*, 1977]. If that is the case, then the signal has propagated about halfway up the main channel. Note that without further evidence, we cannot argue unequivocally that this is indeed the origin of this slope break; we merely wish to illustrate with a field example what such a transient response would look like.

[41] Within the class of detachment-limited models the style of morphologic response in the case of plateau erosion differs markedly depending on the nonlinearity in gradient. Large-scale escarpment retreat occurs under $n \leq 1$. For $n > 1$ the model predicts widespread plateau dissection and the formation of smooth river profiles rather than coherent scarp

retreat. Thus this seemingly innocuous parameter controls the predominance of down wearing (as in the Davis model) versus back wearing (as in King-Penck theory) during plateau erosion. Nonlinearity in the gradient term also has a significant impact on the timing and duration of erosional response and by extension on any resulting sedimentary record. Highly nonlinear models predict a rapid initial response, with strong attenuation of denudation rates over time. Such nonlinear behavior (whether it reflects $n > 1$, the presence of a significant erosion threshold [*Tucker and Slingerland*, 1997; *Snyder et al.*, 2000b] or a transition to transport-limited behavior [*Whipple and Tucker*, 2002; *Baldwin et al.*, 2002]) may help explain evidence for rapid, early denudation followed by relative stability in the evolution of the southern African escarpments [*Cockburn et al.*, 2000].

[42] It seems unlikely that any of the erosion laws that have been proposed are universal, and there remains an important need not only to identify suitable test cases for erosion laws like the ones analyzed here but also to establish the circumstances under which river erosion is limited by transport versus detachment capacity. In general, one would expect transport-limited behavior to be common in orogens underlain by weak lithologies. *Talling* [2000] has recently shown, for example, that rivers in the northern Apennines have Shields stress ratios typical of gravel-bedded alluvial rivers; this finding suggests that these rivers, though actively incising into bedrock, are effectively transport limited. For detachment-limited fluvial systems on resistant bedrock, *Whipple et al.* [2000] developed basic scaling arguments which suggest $n \simeq 1$ for plucking-dominated erosion and $n \simeq 5/3$ for abrasion-dominated erosion. Thus the mode of behavior in any given drainage basin, whether detachment-limited, transport-limited, or somewhere in between, is likely to depend strongly on the rock substrate, as well as on the nature of transport-detachment coupling [*Sklar and Dietrich*, 1998; *Whipple and Tucker*, 2002].

[43] Given the importance of the form of an erosion law for large-scale topography and erosional dynamics, we suggest that future research should focus on testing and refining existing laws. This can be done by several means. First, the theory developed here can be extended to more complex erosion laws that incorporate the role of sediment as an abrasion and/or insulating agent [e.g., *Beaumont et al.*, 1992; *Sklar and Dietrich*, 1998; *Stock and Dietrich*, 1999; *Whipple and Tucker*, 2002] and to flesh out the theoretical implications of stochasticity in discharge and sediment flux [*Tucker and Bras*, 2000]. Second, regions of known and spatially variable uplift and/or erosion rate such as the ones studied by *Snyder et al.* [2000a] and *Kirby and Whipple* [2001] need to be analyzed for the information they contain about relief-uplift/erosion scaling. Finally, case study sites that provide a snapshot of a transient response to a known base level change should be analyzed in order to place constraints on the dynamic response of fluvial systems.

[44] **Acknowledgments.** We are grateful for support from the National Science Foundation (EAR-9725723) and the U.S. Army Research Office (DAAD19-01-1-0615). We thank Peter Talling for sharing data on the Enza River that appears in Table 1 and A. Allen and D. Sansom for drafting assistance. The manuscript benefited greatly from reviews by Alex Densmore and Alan Howard.

References

Adams, J., Large-scale tectonic geomorphology of the Southern Alps, New Zealand, in *Tectonic Geomorphology, Binghamton Symposia in Geomorphology, Int. Ser.*, vol. 15, edited by M. Morisawa and J. T. Hack, pp. 105–128, Allen and Unwin, Concord, Mass., 1985.

Anderson, R. S., Evolution of the Santa Cruz Mountains, California, through tectonic growth and geomorphic decay, *J. Geophys. Res.*, *99*, 20,161–20,179, 1994.

Anderson, R. S., and N. F. Humphrey, Interaction of weathering and transport processes in the evolution of arid landscapes, in *Quantitative Dynamic Stratigraphy*, edited by T. Cross, pp. 349–361, Prentice-Hall, Englewood Cliffs, N. J., 1990.

Baldwin, J. A., K. X. Whipple, and G. E. Tucker, Implications of the shear-stress river incision model for the timescale of postorogenic decay of topography, *J. Geophys. Res.*, *107*, doi:10.1029/2001JB000550, in press, 2002.

Beaumont, C., P. Fullsack, and J. Hamilton, Erosional control of active compressional orogens, in *Thrust Tectonics*, edited by K. R. McClay, pp. 1–18, Chapman and Hall, New York, 1992.

Burbank, D., J. Leland, E. Fielding, R. S. Anderson, N. Brozovic, M. R. Reid, and C. Duncan, Bedrock incision, rock uplift and threshold hillslopes in the northwestern Himalayas, *Nature*, *379*, 505–510, 1994.

California Division of Mines and Geology, Geologic map of California, Death Valley sheet, scale 1:250,000 geologic map, Sacramento, 1977.

Carson, M. A., and D. J. Petley, The existence of threshold hillslopes in the denudation of the landscape, *Trans. Inst. Br. Geogr.*, *49*, 71–95, 1970.

Chase, C. G., Fluvial landsculpting and the fractal dimension of topography, *Geomorphology*, *5*, 39–57, 1992.

Cockburn, H. A. P., R. W. Brown, M. A. Summerfield, and M. A. Seidl, Quantifying passive margin denudation and landscape development using a combined fission-track thermochronology and cosmogenic isotope analysis approach, *Earth Planet. Sci. Lett.*, *179*(3–4), 429–435, 2000.

Dahlen, F. A., and J. Suppe, Mechanics, growth, and erosion of mountain belts, in *Processes in Continental Lithospheric Deformation*, edited by S. P. Clark Jr., B. C. Burchfiel, and J. Suppe, *Spec. Pap. Geol. Soc. Am.*, 218, 161–178, 1988.

Davis, W. M., The geographical cycle, *Geogr. J.*, *14*, 481–504, 1899.

Densmore, A. L., M. A. Ellis, and R. S. Anderson, Landsliding and the evolution of normal-fault-bounded mountains, *J. Geophys. Res.*, *103*, 15,203–15,219, 1998.

Foley, M., Bed-rock incision by streams, *Geol. Soc. Am. Bull. Part II*, *91*, 664–672, 1980.

Foster, G. R., and L. D. Meyer, A closed-form erosion equation for upland areas, in *Sedimentation: Symposium to Honor Professor H. A. Einstein*, edited by H. W. Shen, pp. 12.1–12.19, Colo. State Univ., Fort Collins, 1972.

Gasparini, N. M., G. E. Tucker, and R. L. Bras, Downstream fining through selective particle sorting in an equilibrium drainage network, *Geology*, *27*(12), 1079–1082, 1999.

Gilchrist, A. R., H. Kooi, and C. Beaumont, Post-Gondwana geomorphic evolution of southwestern Africa; implications for the controls on landscape development from observations and numerical experiments, *J. Geophys. Res.*, *99*, 12,211–12,228, 1994.

Hack, J. T., Studies of longitudinal stream profiles in Virginia and Maryland, *U.S. Geol. Surv. Prof. Pap.*, *294-B*, 97 pp., 1957.

Howard, A. D., Simulation model of stream capture, *Geol. Soc. Am. Bull.*, *82*, 1355–1376, 1971.

Howard, A. D., Thresholds in river regimes, in *Thresholds in Geomorphology*, edited by D. R. Coates and J. D. Vitek, pp. 227–258, Allen and Unwin, Concord, Mass., 1980.

Howard, A. D., A detchment-limited model of drainage basin evolution, *Water Resour. Res.*, *30*, 2261–2285, 1994.

Howard, A. D., Badland morphology and evolution: Interpretation using a simulation model, *Earth Surf. Processes Landforms*, *22*, 211–227, 1997.

Howard, A. D., and G. Kerby, Channel changes in badlands, *Geol. Soc. Am. Bull.*, *94*, 739–752, 1983.

Howard, A. D., W. E. Dietrich, and M. A. Seidl, Modeling fluvial erosion on regional to continental scales, *J. Geophys. Res.*, *99*, 13,971–13,986, 1994.

Hurtrez, J. E., F. Lucazeau, J. Lave, and J.-P. Avouac, Investigations of the relationships between basin morphology, tectonic uplift, and denudation from study of an active fold belt in the Siwalik Hills, central Nepal, *J. Geophys. Res.*, *104*, 12,779–12,796, 1999.

King, L. C., Canons of landscape evolution, *Geol. Soc. Am. Bull.*, *64*, 721–752, 1953.

Kirby, E., and K. X. Whipple, Quantifying differential rock uplift rates via stream profile analysis, *Geology*, *29*, 415–418, 2001.

Kirkby, M. J., Modelling some influences of soil erosion, landslides and valley gradient on drainage density and hollow development, *Catena Suppl.*, *10*, 1–14, 1987.

Kooi, H., and C. Beaumont, Escarpment evolution on high-elevation rifted margins: Insights derived from a surface processes model that combines diffusion, advection, and reaction, *J. Geophys. Res.*, *99*, 12,191–12,209, 1994.

Kooi, H., and C. Beaumont, Large-scale geomorphology: Classical concepts reconciled and integrated with contemporary ideas via a surface processes model, *J. Geophys. Res.*, *101*, 3361–3386, 1996.

Molnar, P., and P. England, Late Cenozoic uplift of mountain ranges and global climate change: Chicken or egg?, *Nature*, *346*, 29–34, 1990.

Montgomery, D. R., and W. E. Dietrich, Where do channels begin?, *Nature*, *336*, 232–234, 1988.

Montgomery, D. R., and W. E. Dietrich, Channel initiation and the problem of landscape scale, *Science*, *255*, 826–830, 1992.

Montgomery, D. R., T. B. Abbe, J. M. Buffington, N. P. Peterson, K. M. Schmidt, and J. D. Stock, Distribution of bedrock and alluvial channels in forested mountain drainage basins, *Nature*, *381*, 587–589, 1996.

Oguchi, T., Drainage density and relative relief in humid steep mountains with frequent slope failure, *Earth Surf. Processes Landforms*, *22*, 107–120, 1997.

Ohmori, H., Morphotectonic evolution of Japan, in *Geomorphology and Global Tectonics*, edited by M. A. Summerfield, pp. 147–166, John Wiley, New York, 2000.

Paola, C., P. L. Heller, and C. L. Angevine, The large-scale dynamics of grain-size variation in alluvial basins, 1, Theory, *Basin Res.*, *4*, 73–90, 1992.

Penck, W., Morphological Analysis of Land Forms: A Contribution to Physical Geography, translated by H. Czech and K. C. Boswell, 429 pp., Macmillan, Old Tappan, N. J., 1921.

Reneau, S. L., and W. E. Dietrich, Erosion rates in the southern Oregon coast range: Evidence for an equilibrium between hillslope erosion and sediment yield, *Earth Surf. Processes Landforms*, *16*, 307–322, 1991.

Rigon, R., I. Rodriguez-Iturbe, A. Maritan, A. Giacometti, D. G. Tarboton, and A. Rinaldo, On Hack's law, *Water Resour. Res.*, *32*, 3367–3374, 1996.

Rodriguez Iturbe, I., and A. Rinaldo, *Fractal River Basins: Chance and Self-Organization*, 547 pp., Cambridge Univ. Press, New York, 1997.

Roering, J. J., J. W. Kirchner, and W. E. Dietrich, Evidence for nonlinear, diffusive sediment transport on hillslopes and implications for landscape morphology, *Water Resour. Res.*, *35*, 853–870, 1999.

Rosenbloom, N. A., and R. S. Anderson, Hillslope and channel evolution in a marine terraced landscape, Santa Cruz, California, *J. Geophys. Res.*, *99*, 14,013–14,030, 1994.

Royden, L. H., M. K. Clark, and K. X. Whipple, Evolution of river elevation profiles by bedrock incision: Analytical solutions for transient river profiles related to changing uplift and precipitation rates, *Eos Trans. AGU*, *81*(48), Fall Meet. Suppl., Abstract T62F-09, 2000.

Schmidt, K., and D. Montgomery, Limits to relief, *Science*, *270*, 617–620, 1995.

Seidl, M. A., and W. E. Dietrich, The problem of channel erosion into bedrock, *Catena Suppl.*, *23*, 101–124, 1992.

Seidl, M. A., W. E. Dietrich, and J. W. Kirchner, Longitudinal profile development into bedrock: An analysis of Hawaiian channels, *J. Geol.*, *102*, 457–474, 1994.

Sklar, L., and W. E. Dietrich, River longitudinal profiles and bedrock incision models: Stream power and the influence of sediment supply, in *Rivers Over Rock: Fluvial Processes in Bedrock Channels, Geophysical Monogr. Ser.*, vol. 107, edited by E. Wohl and K. Tinkler, pp. 237–260, AGU, Washington, D. C., 1998.

Slingerland, R., S. D. Willett, and H. L. Hennessey, A new fluvial bedrock erosion model based on the work-energy principle, *Eos Trans. AGU*, *78*(46), Fall Meet. Suppl., F299, 1997.

Snow, R. S., and R. L. Slingerland, Mathematical modeling of graded river profiles, *J. Geol.*, *95*, 15–33, 1987.

Snyder, N. P., K. X. Whipple, G. E. Tucker, and D. J. Merritts, Landscape response to tectonic forcing: DEM analysis of stream profiles in the Mendocino triple junction region, northern California, *Geol. Soc. Am. Bull.*, *112*, 1250–1263, 2000a.

Snyder, N. P., K. X. Whipple, and G. E. Tucker, The influence of a stochastic distribution of storms and a critical shear stress for detachment on the relation between steady-state bedrock channel gradient and rock-uplift rate, paper presented at Annual Meeting, Geol. Soc. of Am., Reno, Nev., 12–16 Nov., 2000b.

Stock, J., and W. E. Dietrich, Valley incision by debris flows: Field evidence and hypotheses linking flow frequency to morphology, *Eos Trans. AGU*, *80*(46), Fall Meet. Suppl., F473, 1999.

Talling, P., Self-organization of river networks to threshold states, *Water Resour. Res.*, *36*, 1119–1128, 2000.

Tarboton, D. G., R. L. Bras, and I. Rodriguez-Iturbe, On the extraction of channel networks from digital elevation data, *Hydrol. Processes*, *5*, 81–100, 1991.

Tucker, G. E., Modeling the large-scale interaction of climate, tectonics, and topography, *Tech. Rep. 96-003*, *Earth Syst. Sci. Cent.*, Pa. State Univ., University Park, 1996.

Tucker, G. E., and R. L. Bras, Hillslope processes, drainage density, and landscape morphology, *Water Resour. Res.*, *34*, 2751–2764, 1998.

Tucker, G. E., and R. L. Bras, A stochastic approach to modeling the role of rainfall variability in drainage basin evolution, *Water Resour. Res.*, *36*, 1953–1964, 2000.

Tucker, G. E., and R. L. Slingerland, Erosional dynamics, flexural isostasy, and long-lived escarpments: A numerical modeling study, *J. Geophys. Res.*, *99*, 12,229–12,243, 1994.

Tucker, G. E., and R. L. Slingerland, Predicting sediment flux from fold and thrust belts, *Basin Res.*, *8*, 329–349, 1996.

Tucker, G. E., and R. L. Slingerland, Drainage basin response to climate change, *Water Resour. Res.*, *33*, 2031–2047, 1997.

Tucker, G. E., F. Catani, A. Rinaldo, and R. L. Bras, Statistical analysis of drainage density from digital terrain data, *Geomorphology*, *36*(3–4), 187–202, 2001a.

Tucker, G. E., S. T. Lancaster, N. M. Gasparini, and R. L. Bras, The Channel-Hillslope Integrated Landscape Development model (CHILD), in *Landscape Erosion and Evolution Modeling*, edited by R. S. Harmon and W. W. Doe III, pp. 349–388, Kluwer Acad., Norwell, Mass., 2001b.

Tucker, G. E., S. T. Lancaster, N. M. Gasparini, R. L. Bras, and S. M. Rybarczyk, An object-oriented framework for hydrologic and geomorphic modeling using triangulated irregular networks, *Comput. Geosci.*, *27*(8), 959–973, 2001c.

van der Beek, P., and J. Braun, Numerical modelling of landscape evolution on geological time-scales: A parameter analysis and comparison with the south-eastern highlands of Australia, *Basin Res.*, *10*, 49–68, 2000.

Weissel, J. K., and M. A. Seidl, Inland propagation of erosional escarpments and river profile evolution across the southeast Australian passive continental margin, in *Rivers Over Rock: Fluvial Processes in Bedrock Channels, Geophys. Monogr. Ser.*, vol. 107, edited by E. Wohl and K. Tinkler, pp. 189–206, AGU, Washington, D. C., 1998.

Whipple, K. X., Fluvial landscape response time: How plausible is steady-state denudation?, *Am. J. Sci.*, *301*, 313–325, 2001.

Whipple, K. X., and C. R. Trayler, Tectonic control of fan size: The importance of spatially variable subsidence rates, *Basin Res.*, *8*, 351–365, 1996.

Whipple, K. X., and G. E. Tucker, Dynamics of the stream power river incision model: Implications for height limits of mountain ranges, landscape response timescales and research needs, *J. Geophys. Res.*, *104*, 17,661–17,674, 1999.

Whipple, K. X., and G. E. Tucker, Implications of sediment-flux-dependent river incision models for landscape evolution, *J. Geophys. Res.*, *107*(B2), 10.1029/2000JB000044, 2002.

Whipple, K. X., E. Kirby, and S. H. Brocklehurst, Geomorphic limits to climate-induced increases in topographic relief, *Nature*, *401*, 39–43, 1999.

Whipple, K. X., G. S. Hancock, and R. S. Anderson, River incision into bedrock: Mechanics and relative efficacy of plucking, abrasion, and cavitation, *Geol. Soc. Am. Bull.*, *112*, 490–503, 2000.

Willett, S. D., C. Beaumont, and P. Fullsack, Mechanical model for the tectonics of doubly vergent compressional orogens, *Geology*, *21*, 371–374, 1993.

Willgoose, G. R., A physical explanation for an observed area-slope-elevation relationship for catchments with declining relief, *Water Resour. Res.*, *30*, 151–159, 1994.

Willgoose, G. R., R. L. Bras, and I. Rodriguez-Iturbe, A physically based coupled network growth and hillslope evolution model, 1, Theory, *Water Resour. Res.*, *27*, 1671–1684, 1991.

G. E. Tucker, School of Geography and the Environment, Oxford University, Mansfield Road, Oxford OX1 3TB, UK. (greg.tucker@geog.ox.ac.uk)

K. X. Whipple, Department of Earth, Atmospheric, and Planetary Science, Massachusetts Institute of Technology, Cambridge, MA 02139-4307, USA. (kxw@mit.edu)